Absorption Spectroscopy of Solid-Phase Fullerene C 60 between 1.65 and 2.78 μm

Shubhadip Chakraborty, Karine Demyk, Ludovic Biennier, Robert Georges

Absorption Spectroscopy of Solid-Phase Fullerene C_{60} between 1.65 and 2.78 μm

Shubhadip Chakraborty,*,† Karine Demyk,‡ Ludovic Biennier,† and Robert Georges*,†

†*Institut de Physique de Rennes, UMR CNRS 6251, Université de Rennes 1, Campus de Beaulieu, 35042 Rennes Cedex, France*

‡*Institut de Recherche en Astrophysique et Planétologie, Université de Toulouse, CNRS, CNES, 9 Av. du Colonel Roche, 31028 Toulouse Cedex 4, France*

E-mail: shubhadip.chakraborty@univ-rennes1.fr; robert.georges@univ-rennes1.fr

Abstract

Fullerenes are the largest molecules identified so far in the interstellar medium. The spectroscopic properties of C_{60} and its charge variants, have been extensively studied in the mid-infrared, near ultraviolet and visible regions. On the other hand, the near infrared (NIR) spectral region has remained relatively unexplored, in particular for neutral C_{60}. Here we report the first measurements of the absorption spectra of solid C_{60} from 6052 to 3596 cm^{-1} (from 1.65 to 2.78 μm) recorded over the 11 to 300 K temperature range. NIR spectra of C_{60} microcrystals embedded in solid KBr were measured using a low temperature helium cryocooling setup coupled to a Fourier transform infrared spectrometer. The observed spectra of C_{60} from 1.65 to 2.78 μm show highly structured absorption features. Compared to isolated molecules, the lower symmetry of C_{60} microcrystals optically activates many fundamental vibrational modes which combine (up to 4 quanta) and contribute to the rich observed spectrum. Quantum chemical calculations and group theoretical analysis were performed for a tentative assignment of the observed combination and overtone bands to the calculated transitions of both regions by identifying the IR active T_{1u} symmetries. 3895 combination and overtone transitions were calculated in the region between 1.65 and 2.78 μm amongst which 1862 transitions belong to the IR active T_{1u} symmetry, expected to be observed in the absorption spectrum of gas-phase C_{60}. This work offers some guidance for future low temperature gas-phase NIR absorption spectroscopic studies of C_{60}. Measurements of vibrational overtone bands of C_{60} are extremely timely for the identification of the carriers of NIR DIBs (Diffuse Interstellar Bands) in the context of the upcoming launch of the James Webb Space Telescope.

Keywords

Fullerene, Infrared spectroscopy, Astrochemistry, Quantum Chemistry, Diffuse interstellar bands

1 Introduction

Fullerenes were discovered in laboratory experiments using laser-induced vaporization of graphite, aimed at understanding how long carbon chains could form in the circumstellar envelope of dying stars.[1] Over the last decades, fullerenes and their derivatives have been the subject of intense research, as much for their chemical and physical properties as for their technological applications. Following bulk-production of fullerenes by a method developed by Krätschmer et al.[2], major efforts have been made to investigate the spectroscopic fingerprints of C_{60}, especially in the mid-infrared. In the solid-phase, absorption studies have been conducted by embedding C_{60} crystals in KBr[3] or in films[4,5] maintained at low temperature. Some experiments in which C_{60} was trapped in a rare-gas matrix have also been performed. Fulara et al.[6] reported the IR spectrum of C_{60} isolated in a Ne matrix. Sogoshi et al.[7] performed some experiments in a para-hydrogen matrix while more recently Wakabayashi et al.[8] reported the IR spectra of isotopically substituted C_{60} in a para-hydrogen matrix. In the gas-phase, absorption measurements of neutral C_{60} were hindered by the huge vibrational partition function of C_{60}, even at room temperature,[9] that limits the signal from the ground state. It is only very recently that Changala et al.[10] managed to successfully record the IR absorption spectrum at 8.5 μm of cold C_{60} in the gas-phase using a collisional cooling cell coupled with frequency comb spectroscopy. The gas-phase IR spectra of C_{60} was also recorded in emission by Nemes et al.[11] over the 879-1212 K temperature range and to date, this is the only available broadband gas-phase data for neutral C_{60}. In parallel to the experiments, a few theoretical harmonic frequency calculations on C_{60} were performed, primarily focusing on the mid-infrared region.[12,13] However, no attempt has been made for a complete anharmonic frequency calculation of C_{60} including various resonances even in the mid-infrared region.

In 2010, twenty-five years after their accidental discovery during laboratory astrophysics experiments, their presence in space was finally observed. The fullerenes C_{60} and C_{70} were identified in the Tc1 planetary nebula[14,15] and the NGC 7023 and 2023 reflection nebu-

lae[16] through their mid-infrared emission features at 7.0, 8.5, 17.4 and 18.9 μm. Since then, fullerenes have been detected in various astronomical objects ranging from diffuse clouds,[17] evolved stars,[15,18–21] star forming regions[22,23] to photodissociation regions.[24] In spite of these series of positive detections, their presence remains rare. It is estimated that only a small fraction of gas-phase carbon is locked in the form of C_{60} fullerene in the interstellar medium (ISM).[17] Notably, the physical and chemical routes leading to the formation of fullerenes, which include bottom-up and top-down pathways, remain open to debate.[25–27] Photo-chemistry,[28] photo-dynamics[29] but also shock processing[30,31] studies of C_{60} aim to shed light on this issue.

Recently, the presence of C_{60}^+ was firmly established in diffuse clouds through an observed match between its electronic spectrum and a few DIBs.[32,33] The approach was based on the photo-fragmentation of C_{60}^+−He clusters confined in a cryogenic radiofrequency multipole ion trap. This work confirmed the hypothesis proposed by Foing and Ehrenfreund[34] based on low-temperature Ne matrix-isolation spectra obtained by Fulara et al.[6]. DIBs are broad absorption features (with bandwidths varying between 2 and 80 cm^{-1}) predominantly covering the 0.4 to 0.9 μm range in the spectra of reddened stars.[35–38] The original DIB spectral window has been progressively extended to the NIR range through several observational studies.[39–47] Primarily driven by the PAH-DIB hypothesis,[48,49] the matrix isolated NIR spectra of a few ionic PAHs were recorded and several electronic transitions between 0.7 and 2.5 μm spectral range were measured.[50] Spectral shifts in the position of the rovibronic bands, induced by the interaction of the isolated PAHs with the matrix, however prevented decisive identification of the NIR DIBs observed by Cox et al.[42]. Barring electronic transitions, the NIR spectral region is also associated with higher order vibrational transitions[51] which have been less scrutinized in the context of laboratory astrophysics.

The identification of C_{60}^+ as the carrier of five electronic NIR DIBs inevitably raised the possibility of other fullerene species as potential DIB carriers. In an earlier study, García-Hernández and Díaz-Luis[52] searched for the three strong electronic transitions of C_{60} at $\sim$

3760, 3980 and 4024 Å in two planetary nebulae (PNe) Tc1 and M 1-20 in proximity to the band positions measured in the laboratory in rare gas matrices at low temperatures.[53] Surprisingly, none of the PNe showed the transitions in the expected wavelength range. According to Cami[54], neutral C_{60} is unlikely a carrier of visible strong DIBs as this would require a too large fraction of cosmic carbon to be locked up in this species. The non-observation of C_{60} did not however, question the fact that a significant fraction of this stable molecule is expected to be neutral. Bakes and Tielens[55] had inferred that in the diffuse ISM $\sim$ 60% of C_{60} is in the neutral form, $\sim$ 10% is in the cationic and $\sim$ 30% is in the anionic form. In a more recent work, Berné et al.[17] reported the observation of neutral C_{60} in the diffuse ISM and in a star forming region using both emission and absorption measurements. They derived a neutral to ion ratio in between 0.15 and 2.

The major goal of this paper is to provide the first spectroscopic data of neutral C_{60} from 1.65 to 2.78 μm at various temperatures and to give a tentative assignment to the observed bands to the calculated transitions using quantum chemical calculations. This work paves the way for the future gas-phase study of C_{60} using an ultra-sensitive absorption spectrometer coupled with a hypersonic source developed recently.[56,57]

The paper is structured as follows: in Section 2 we provide the experimental and theoretical methodology employed in this work. In Section 3 we present our results and discuss them. In Section 4, we provide some insights for gas-phase spectroscopy of C_{60} and discuss astrophysical implications. Finally, in Section 5 we wrap-up with conclusions.

2 Methodology

2.1 Experimental Details

Fullerene C_{60} used in this experiment was purchased from SES Research (99.5% purity) and was used without further purification. About 52.09 mg of C_{60} was mixed with $\sim$ 200 mg of KBr (FTIR grade 98%) in an agate mortar and was ground thoroughly for 15 minutes.

The mixture was put in a hydraulic press and was pressed under 10 tonnes of pressure for 5 minutes to form a pellet. The diameter and thickness of the pellet was 12.76 mm and 0.85 mm, respectively. The concentration of C_{60} in the pellet was 6.66×10^{-4} mol/cm^3. A blank pellet containing $\sim$ 200 mg of KBr was prepared in the same way without C_{60} .

The infrared spectra of blank and C_{60} sample pellets were recorded from 6052 to 3596 cm^{-1} (1.65 to 2.78 μm) with the ESPOIRS apparatus at the IRAP laboratory in Toulouse[58,59] from 11 to 300 K with an increasing temperature step of 50 K. A smaller temperature step size of 10 K was used near the phase transition temperature ($\sim$ 260 K) of C_{60}. The transmittance spectrum at each specific temperature was calculated by dividing the sample spectrum with the background spectrum at that temperature. The spectral resolution was kept at 4 cm^{-1} and the acquired interferograms were averaged over 256 scans to increase the signal-to-noise ratio. All spectra were processed using the OPUS suite of programs provided by Bruker optics. Local linear continua were subtracted from the observed spectra at each temperature using the same anchor points for regions I and II (see Figure 1).

The ESPOIRS setup consists of a Bruker Vertex 70 vacuum FTIR spectrometer equipped with multiple sample and detector compartments. For this experiment, a CaF_2 beamsplitter and a room temperature, deuterated triglycine sulfate (DLaTGS) detector was used. This setup is coupled with a helium cryo-cooling device. The optical bench of the spectrometer is pumped via a primary pump while the cryostat in which the sample was placed was pumped using a turbomolecular pump. The pressure inside the sample compartment was brought down to $\sim 10^{-5}$ mbar before turning on the cryo-cooler. By lowering the temperature, the pressure dropped to 10^{-7} mbar. The experimental temperature was set using a Lakeshore temperature controller.

2.2 Theory

The icosahedral fullerene C_{60} molecule belongs to the I_h symmetry group and possesses 46 normal modes of which only 4 are infrared active (T_{1u} symmetry), 10 are Raman active and

the remaining 32 are silent modes. However, in the crystal, the intermolecular interactions reduce the local symmetry of the fullerene cage, leading to very efficient activation of all the silent modes, that can then be seen both through infrared and Raman spectroscopy.[60] In addition, one has to consider the so-called isotopically activated modes. In natural fullerene, the abundance of the isotopologue $^{13}C^{12}C_{59}$ is about 37.5%, which is far from being negligible. It has been demonstrated that the silent modes are also activated by the presence of the ^{13}C isotope in the molecule which reduces its symmetry from I_h to C_s.[61] Considering these two effects, we therefore decided to compute all the possible combination and overtone bands falling in the observed region as all of them can contribute to the infrared spectrum.

The Hessian matrix at the optimized geometry of C_{60} was calculated using the B3LYP level of theory in conjunction with the 6-311G* basis set in the Cartesian framework. Diagonalization of the mass-weighted Cartesian Hessian matrix gives the harmonic frequencies ($\nu_{unscaled}$) as listed in Table S1 (cf. supporting information). Then, instead of considering the anharmonic effects by scaling the harmonic frequencies with some ad hoc scale factor, as done by Schettino et al.[12], an inhouse python program[62] was employed to establish a linear regression between the calculated and the reported experimental frequencies[5,12] (cf. Table S1). For that, we used the assignment of the modes provided by Schettino et al.[12]. Considering only the Raman (A_g, H_g) and infrared (T_{1u}) active modes, our approach leads to a Root-Mean-Square (RMS) of 4.8 cm^{-1}, very similar that of 4.6 cm^{-1} obtained by Schettino et al.[12] However, our approach leads to a better RMS of 5.5 cm^{-1} (versus 6.6 cm^{-1} for Schettino et al.[12]) by considering the complete set of 46 fundamental modes (Raman, infrared and silent modes).

As the NIR spectrum of neutral C_{60} from 1.65 to 2.78 μm is dominated by the vibrational transitions due to $\Delta v = 3$ and 4 quanta, we then computed all possible 3- and 4-quanta combination and overtone transitions in the ranges of 6050 to 5565 and 4765 to 3596 cm^{-1} (cf. Table S2 and S3). We did not include in our calculation, the various anharmonic resonances such as Fermi and Darling Dennison resonances which can shift the interacting vibrational

bands by several cm^{-1}. We also did not calculate the different hot bands, negligible at very low temperatures though not at room temperature, for which the population of the lowest vibrational level located at 264 cm^{-1} is about 1.4 times greater than in the ground state.

In the gas-phase, the modes of C_{60} which are activated by the intermolecular interactions specific to the crystal will disappear. The isotopically activated modes will remain but their overall infrared intensity was estimated by Schettino et al. [12] to be only 3.4% that of the T_{1u} derived modes. This means that, in the framework of a future infrared spectroscopic study or detection of the C_{60} molecule in the gas-phase, it is important to distinguish the IR active modes which are dominating the infrared absorption spectrum, that is to say those which are characterized by at least one T_{1u} symmetry element. We performed a group theoretical analysis of the calculated combination modes of T_{1u} symmetry using a standard quantum chemical approach,[63] as listed in Tables S2 and S3. The theoretical methodologies have been described in detail in the supporting information.

3 Results and Discussion

3.1 NIR spectrum of C_{60}

In Figure 1, we present the absorption spectra of C_{60} at 11 and 300 K ranging from 6052 to 3596 cm^{-1}. Strong and marked spectral features are noticed between 4765 and 3596 cm^{-1} (Region I) while several weak absorption features are distributed over the 6052 to 5565 cm^{-1} region (Region II). A quick look shows no significant change in the 11 and 300 K spectra. A closer observation however, reveals slightly sharper and more intense peaks at 11 K. A combination band of water is observed at 5275 cm^{-1} (1.89 μm) (see Figure 1) reflecting a minor moisture contamination in the measured pellet.

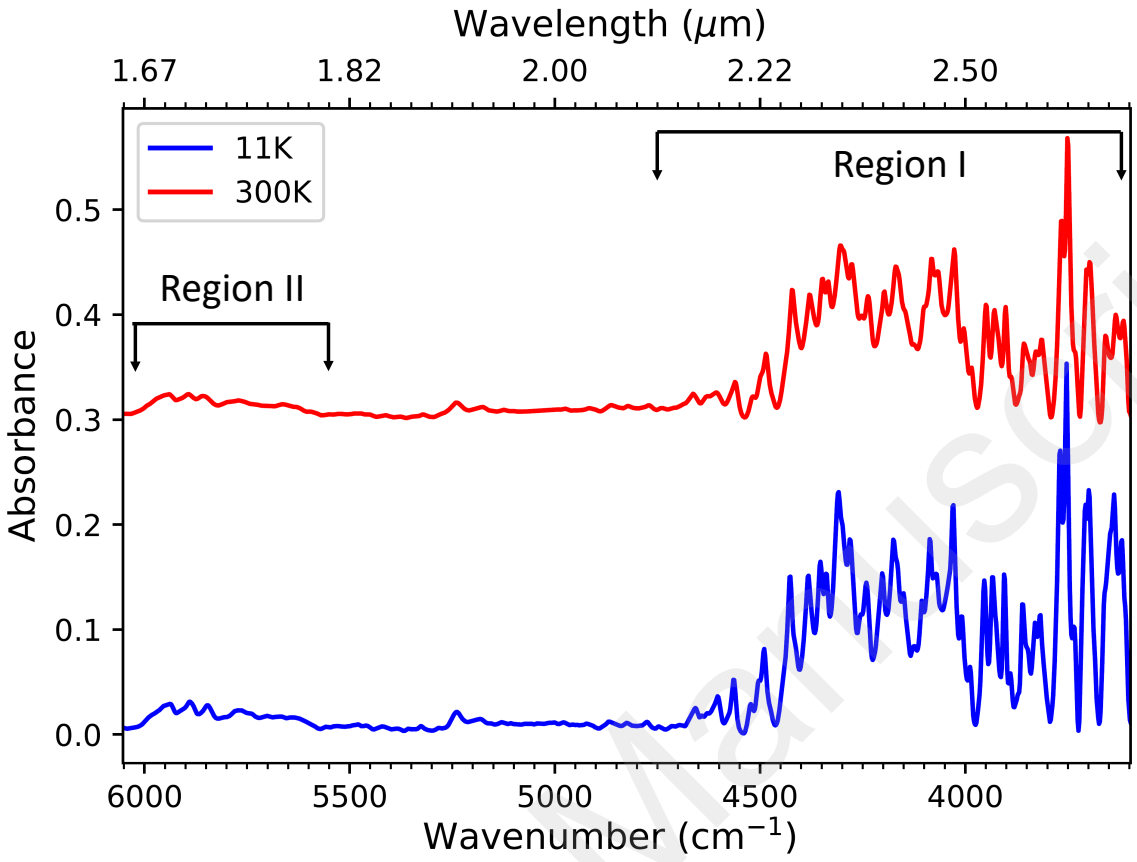

Figure 1: Variable temperature NIR spectra of C_{60} from 6052 to 3596 cm^{-1}(from 1.65 to 2.78 μm). Region I and II correspond to the spectral range from 4765 to 3596 and from 6052 to 5565 cm^{-1}, respectively.

In the left and right panels of Figure 2, we present the absorption spectra of C_{60} from 4765 to 3596 and from 6052 to 5565 cm^{-1} ranging from 11 to 300 K, respectively. The observed spectra contain many peaks and shoulders. Bands of Region I are more structured than those in Region II, being comparatively less resolved with several humps and shoulders. The positions of the peak maxima of the bands of both regions and their relative absorbance values at 11 K are listed in Table 1. There are 39 distinct absorption bands in Region I. On the other hand, in Region II, three bands dominate at 5937.4, 5889.9 and 5846.6 cm^{-1}. Apart from these three, six less isolated absorption features are observed below 5840 cm^{-1}.

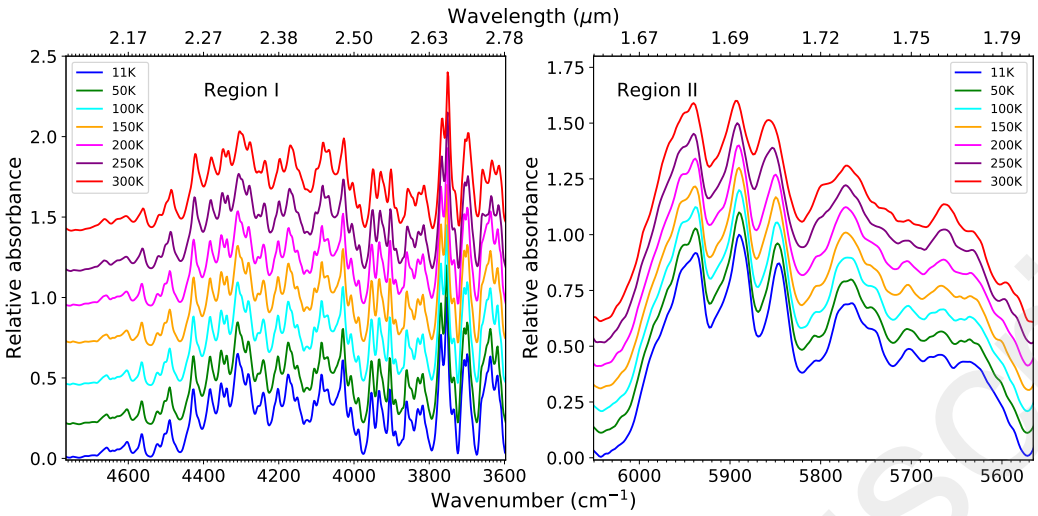

Figure 2: Variable temperature NIR spectra of C_{60} in Region I (from 4765 to 3596 cm^{-1}) and Region II (from 6052 to 5565 cm^{-1}) from 11 to 300 K. A vertical offset has been added to each spectrum for clarity. Enlarged spectra at 11 K for both region I and II are shown in Figs 3 and 4

Table 1: Experimental band positions and their relative absorbances of C_{60} between 6052 and 3596 cm^{-1} at 11 K.

	Region I															Region II		
No	Position (cm^{-1})	Rel. Abs.	No	Position (cm^{-1})	Rel. Abs.	No	Position (cm^{-1})	Rel. Abs.	No	Position (cm^{-1})	Rel. Abs.	No	Position (cm^{-1})	Rel. Abs.	No	Position (cm^{-1})	Rel. Abs.
1	4693.0	0.02	10	4353.2	0.5	19	4124.8	0.2	28	3904.9	0.4	37	3699.6	0.6	1	5937.4	0.9
2	4658.1	0.07	11	4338.8	0.4	20	4105.6	0.4	29	3891.1	0.2	38	3638.6	0.6	2	5889.9	1.0
3	4603.0	0.1	12	4309.4	0.7	21	4086.3	0.5	30	3860.1	0.4	39	3619.4	0.5	3	5846.6	0.9
4	4565.1	0.2	13	4281.0	0.5	22	4071.9	0.4	31	3830.1	0.3				4	5806.6	0.4
5	4523.3	0.09	14	4254.3	0.3	23	4030.2	0.6	32	3817.8	0.3				5	5769.1	0.7
6	4504.1	0.2	15	4241.4	0.4	24	4008.8	0.3	33	3769.1	0.8				6	5740.3	0.6
7	4490.7	0.3	16	4202.4	0.4	25	3988.9	0.2	34	3754.2	1.0				7	5702.8	0.5
8	4427.6	0.4	17	4175.1	0.5	26	3953.7	0.4	35	3735.9	0.3				8	5667.9	0.5
9	4382.7	0.5	18	4151.6	0.4	27	3933.3	0.4	36	3707.6	0.6				9	5637.8	0.4

3.2 Spectral interpretation of the bands in Regions I and II

Wang et al. [4] previously recorded the IR spectrum of a C_{60} film deposited on a KBr substrate at 300 K in the range from 4000 to 400 cm^{-1}. To date, this is the only study where the higher order vibrational transitions (up to 2 quanta) of C_{60} have been assigned, though these assignments were questioned by the more recent study by Schettino et al. [12]. Along with the 4 IR active fundamental modes, they identified 98 two-quanta combination transitions in the 4000-400 cm^{-1} range. They simulated two bands at 4287.6 and 3548.7 cm^{-1} that were

assigned to the third overtone of the two highest frequency IR active fundamental modes of C_{60} belonging to T_{1u} symmetry. However, they did not observe any bands above 3500 cm^{-1}. In contrast, we could observe 15 peaks between 3500 and 4000 cm^{-1}, probably due to a better signal-to-noise ratio.

Each of the clearly identifiable peaks observed in our laboratory spectra is in fact made up of dozens of transitions connecting the vibrational ground state and the thermally populated excited vibrational states to many upper combination and overtone vibrational modes, eventually interacting via Fermi or Darling-Dennison resonances. These transitions overlap to form a "global" peak which cannot be interpreted simply on the sole basis of a calculation of the position of the vibrational energy levels and without taking into account the intensities of the different transitions involved. In order to comment on the intensity, it is important to include the higher order dipole derivatives of the Taylor series expansion of the dipole moment surface. This is a huge task which is beyond the scope of the present work. In Figures 3 and 4 we present however, the calculated cold band positions for Regions I and II, together with the experimental spectrum of C_{60} recorded at 11 K for which the contribution of the hot bands is totally absent. These calculations do not reveal any particular grouping of energy levels in packets which could explain the presence of the well identified absorption peaks. Indeed, accidental vibrational degeneracies are responsible for the vibrational polyad structure of highly symmetric molecules, such as methane for example.

Our calculations show that the bands appearing between 1.65 and 2.78 μm must have at least 3- or 4-quanta states. Due to its lower energy, Region I is populated with both 3 and 4 quanta states. Since the oscillator strengths of transitions starting from 3-quanta states are higher than that starting from 4-quanta states, we presume that the observed bands in Region I are primarily due to 3-quanta transitions. For Region II, our calculations predict only 4-quanta transitions and nullify the possibility of 3-quanta states due to energy mismatch. However, there could be 5-quanta states in Region II but the associated oscillator strengths will be too weak to show up in this region. We simulated a total of 2098 3-quanta

and 1797 4-quanta transitions in Region I and II, respectively and these are marked with green vertical lines in Figures 3 and 4. In total, our calculation predicts 3895 transitions in the spectral range from 1.65 to 2.78 μm

Surprisingly, the overall shape of the spectrum hardly changes from 11 to 300 K while the contribution of a large number of hot bands is expected at room temperature. Amongst the 46 normal modes of C_{60}, 7 of them have vibration frequencies below 500 cm^{-1} and should contribute significantly to the room temperature spectrum. A closer look reveals that the positions of the peaks actually evolve with temperature, either towards low or high wavenumbers depending on the bands. In the supporting information we report the evolution of a few peaks with temperature. At room temperature, the main peaks are broader while their amplitude is smaller. The peak broadening results in the overlapping contribution of hot bands shifted by vibrational anharmonicities, while the smaller amplitude relates to the population of the ground state which is smaller at room temperature.

Interestingly, we observe a more pronounced shift for a number of peaks at 260 K which nicely confirms the observation of Narasimhan et al.[64] and van Loosdrecht et al.[65], being interpreted as due to a crystal structure change from the face-centered-cubic (*fcc*) to the simple cubic (*sc*) structure (from room to low temperature).

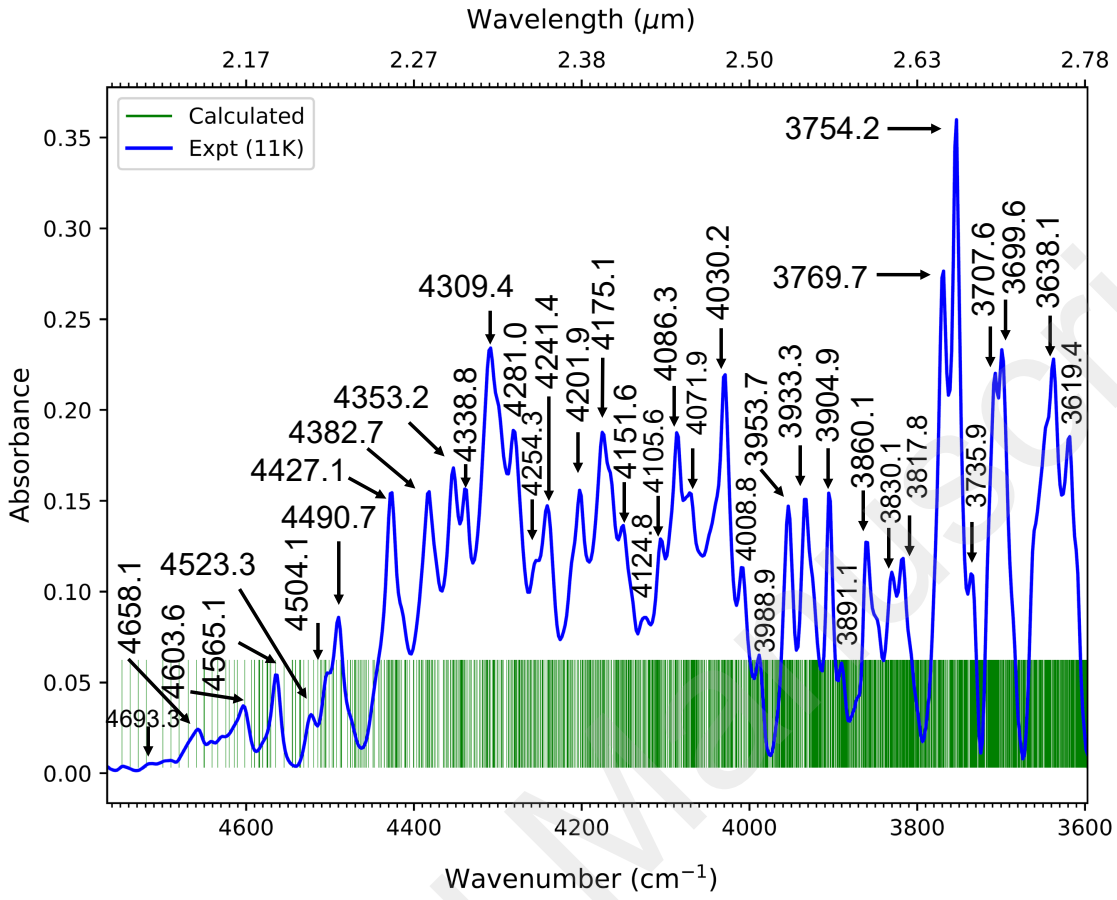

Figure 3: Experimental NIR spectrum of C_{60} at 11 K together with the position of the combination and overtone bands computed at 0 K and limited to 3 quanta. The green vertical lines show a total of 2098 combination and overtone transitions computed in this region. Peak positions at the band maximum are marked in the figure.

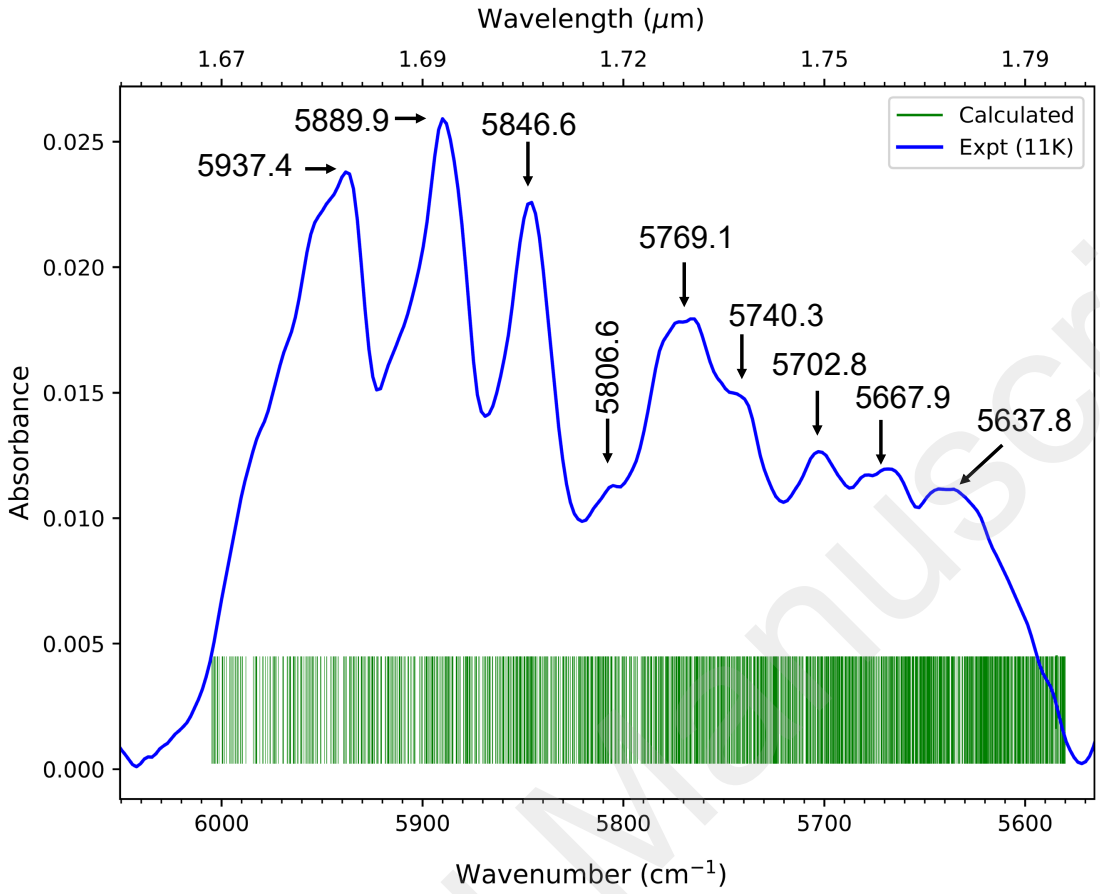

Figure 4: Experimental NIR spectrum of C_{60} at 11 K together with the position of the combination and overtone bands computed at 0 K and limited to 4 quanta. The green vertical lines show a total of 1797 combination and overtone transitions computed in this region. Peak positions at the band maximum are marked in the figure.

4 Insights for gas-phase spectroscopy of C_{60} and astrophysical implications

A key issue for the detection of molecular C_{60} in the cold ISM in the NIR is how different the gas-phase spectra would be from the solid phase? So far, the infrared data recorded in the gas-phase is very scarce. Apart from the IR active mode at 1180 cm^{-1} recorded recently by Changala et al.[10] at $\sim$ 135 K by absorption spectroscopy the only study dealing with the gas-phase spectroscopy of C_{60} is that of Nemes et al.[11]. They observed the 4 IR active T_{1u}

modes at 1407.2, 1165.8, 570.0 and 527.5 cm^{-1} by emission spectroscopy of C_{60} vapor heated to 1083 K. They also observed 14 additional weak features between 2170 and 951 cm^{-1} but could not assign them. The weak feature they observed at 1538 cm^{-1} has only been recently assigned to a 2-quanta combination transition involving an H_g fundamental mode at 772 cm^{-1} and a G_u fundamental mode at 764 cm^{-1}.[66,67] None of these two modes are IR active, however their 2-quanta combination possesses a T_{1u} symmetry element and is therefore active in the infrared. In particular, this band was also observed in the astronomical spectrum of C_{60} by Cami et al.[14]. Of very valuable help, the data produced by Nemes et al.[11] are nevertheless affected by a very significant contribution of hot bands responsible for a shift of several cm^{-1} of the peak maxima, as can be seen by comparing the values of their reported T_{1u} active modes with those deduced from combined ab initio and solid phase studies.

We believe that the solid phase spectra produced at very low temperature in this work can give some interesting insights for a detection of C_{60} in the gas-phase. What changes are going to take place from the solid to the gas-phase? Firstly, the weak transitions due to the silent modes activated by intermolecular interactions will disappear. Secondly, the peak splitting due to the removal of degeneracy of the IR active modes induced by the symmetry lowering associated with the *sc* crystal phase[65] will no longer exist, and a number of low intensity satellite peaks will also disappear. On the other hand, the isotopically activated modes will be present and will continue to produce IR transitions of weaker intensity. In addition, we expect that the absorption bands in the NIR will be broadened by strong intramolecular resonances coupling multiple high-order vibrational states, preventing access to their rotational structure. In conclusion, the NIR gas-phase spectrum is expected to be slightly more decongested with sharper peaks.

Therefore, in support of our future low temperature, gas-phase absorption spectroscopy of C_{60} we have computed the IR active combination and overtone transitions in the region between 1.65 and 2.78 μm arising from all the 46 fundamental modes. Regions I and II contain 986 and 876 combination and overtone transitions of T_{1u} symmetry element, respectively.

We anticipate these 1862 transitions will appear in the absorption spectrum of gas-phase C_{60} , however those involving at least one or more quanta of the four IR active fundamentals (c.f. Table S1) will have the strongest intensity. Figure 5 presents a statistical analysis of the calculated bands by considering all posssible combination and overtone bands of C_{60} in the solid-phase together with those expected to be observed in the gas-phase (having T_{1u} symmetry). From Figs. 5 (a) and (b) it is evident that approximately 50% of the calculated transitions in the solid-phase under each bin, have T_{1u} symmetry and therefore will be observed in the gas-phase. It can be seen that the density of 3-quanta states decreases from 3596 to 4765 cm^{-1} and the density of the 4-quanta states peaks between 5600 and 5700 cm^{-1}.

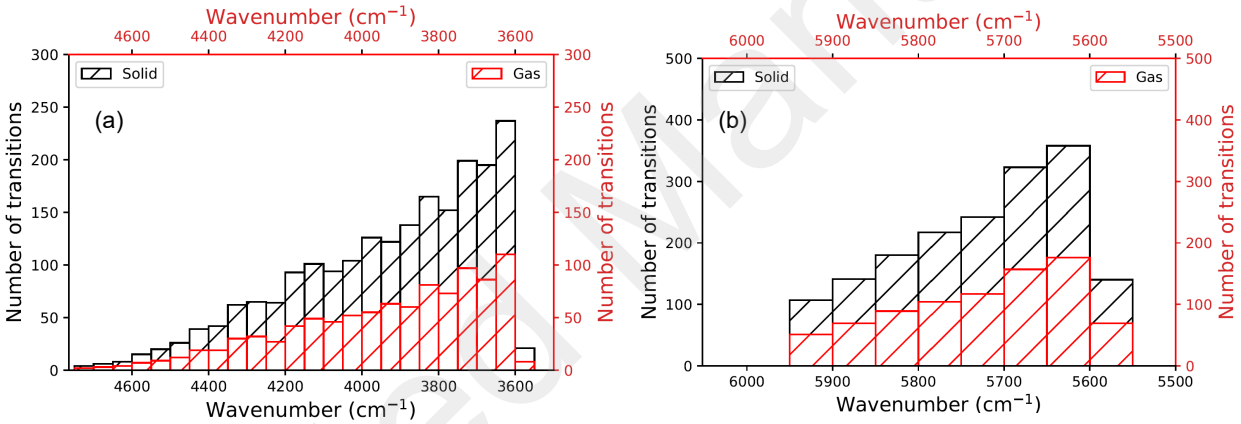

Figure 5: Density of 3- and 4-quanta transitions of C_{60} in Region I and II. Black and red histograms shows the number of calculated transitions in the solid and gas-phase, respectively.

A decisive identification of higher quanta vibrational transitions of C_{60} and the NIR DIBs in the astronomical absorption spectra can be made upon comparison with the band positions obtained from the gas-phase absorption spectroscopy. In Table 2 we have listed a few observed DIBs in the near infrared range together with our experimental band positions. We note that three DIBs observed at 16588, 17803 and 21887 Å by Cox et al. [42] are only 4, -66 and 18 Å away from our solid-phase measurement. Two more DIBs observed by Galazutdinov et al. [47] at 21274 and 23919 Å are 32 and -37 Å away from the data reported in this work. So far, all DIBs are observed using ground based telescopes and their detection relies on a good subtraction of telluric features. Hence, more NIR DIBs between 10,000 to 25,000 Å could be hidden in the noise and not retrieved by the telluric line removal process. [42] The upcoming launch of the James Webb Space Telescope with its onboard NIRSpec instrument, will greatly increase the sensitivity of the observations in the NIR region without contribution from telluric atmospheric lines. It should allow new NIR DIBs to be detected in various astronomical environments.

Table 2: Experimental band positions of neutral C_{60} at 11 K (cf. Fig.3 and Fig.4) and the observed NIR DIBs in various astronomical objects. The experimental band positions reported in this work were obtained from the solid phase study.

λ_{expt} (Å)	λ_{obs} (Å)	λ_{expt} (Å)	λ_{obs} (Å)
	16567[a]	21724	
	16578[a]		21842[a]
16592	16588[a]		21887[a]
16842		21905	
16978		22107	
17104		22201	
17221		22268	
17333			22144[b]
17420		22585	
17535		22816	
17643		22971	
17737		23047	
	17803[a]	23205	
	19940[b]	23359	
	20427[a]	23505	
	20877[b]	23577	
	21274[b]	23795	
	21387[a]		23919[b]
21467		23951	

5 Conclusions

This study aims to provide guidance for future gas-phase absorption spectroscopy of neutral C_{60}. Our work is a first building block towards the systematic exploration of overtone and combination bands of neutral C_{60}, in connection with the C_{60}-DIBs hypothesis. In this framework we have measured the NIR spectrum of C_{60} from 11 to 300 K between 1.65 and 2.78 μm and the observed bands are tentatively assigned to 3- and 4-quanta combination and overtone transitions. We computed a total of 3895 combination and overtone transitions amongst which 1862 transitions have IR active T_{1u} symmetry. We expect them to be observed in the spectrum of gas-phase C_{60}. Due to the presence of a large number of

[a]Cox. et al. 2014
[b]Galazutdinov et al. 2017

normal modes, a complete anharmonic calculation including various resonances of C_{60} has not yet been attempted, even in the frequency range from 4000 to 400 cm^{-1}. The theoretical methodology presented in this work does not compute the intensities of the high order vibrational transitions and the associated anharmonic effects but can be considered as the best effort to interpret the higher order vibrational transitions of C_{60}. Although five frequencies observed in this work are close to the observed DIBs at 16588, 17803, 21887, 21274 and 23919 Å, conclusive evidence can only be established with the aid of gas-phase absorption spectra.

6 Acknowledgements

This work was funded by the Indo-French Center for the Promotion of Advanced Research (CEFIPRA/IFCPAR) under project 6005-N and the Programme National "Physique et Chimie du Milieu Interstellaire" (PCMI) of CNRS/INSU with INC/INP co-funded by CEA and CNES. We thank Prof. Manuel Goubet from the Université de Lille and Dr. Rosine Lallement from GEPI, Observatoire de Paris for reading the manuscript and providing some insightful comments. SC thanks Dr. Sumanta Mukherjee from IBM India Research, for helping to develop the matrix minimization algorithm. SC is grateful to Dr. Subrata Banik from the School of Chemistry and Biotechnology, SASTRA University, India for many helpful discussions. SC thanks Dr. Christine Joblin, from the Institut de Recherche en Astrophysique et Planétologie, Toulouse for many fruitful discussions on C_{60} and its astrophysical relevance. We finally thank the referees who greatly contributed improving of the manuscript.

Supporting Information Available

- Theoretical methodology
- Table S1 Theoretical and experimental frequencies of C_{60}

- Effect of temperature on the observed band position
- Table S3 1797 combination and/or overtone bands of C_{60} between 6005-5580 cm^{-1}
- Table S4 2098 combination and/or overtone bands of C_{60} between 4765-3596 cm^{-1}

References

(1) Kroto, H. W.; Heath, J. R.; O'Brien, S. C.; Curl, R. F.; Smalley, R. E. C_{60}: Buckminsterfullrene. *Nature* **1985**, *318*, 162–163.

(2) Krätschmer, W.; Lamb, L. D.; Fostiropoulos, K.; Huffman, D. R. Solid C_{60}: A New Form of Carbon. *Nature* **1990**, *347*, 354–358.

(3) Graja, A.; Świetlik, R. Temperature Study of IR Spectra of Some C_{60} Compounds. *Synth. Met.* **1995**, *70*, 1417 – 1418.

(4) Wang, K. A.; Rao, A. M.; Eklund, P. C.; Dresselhaus, M. S.; Dresselhaus, G. Observation of Higher-Order Infrared Modes in Solid C_{60} Films. *Phys. Rev. B* **1993**, *48*, 11375–11380.

(5) Martin, M. C.; Fabian, J.; Godard, J.; Bernier, P.; Lambert, J. M.; Mihaly, L. Vibrational Study of ^{13}enriched C_{60} Crystals. *Phys. Rev. B* **1995**, *51*, 2844–2847.

(6) Fulara, J.; Jakobi, M.; Maier, J. P. Electronic and Infrared Spectra of C_{60}^{+} and C_{60}^{-} in Neon and Argon Matrices. *Chem. Phys. Lett.* **1993**, *211*, 227 – 234.

(7) Sogoshi, N.; Kato, Y.; Wakabayashi, T.; Momose, T.; Tam, S.; DeRose, M. E.; Fajardo, M. E. High-Resolution Infrared Absorption Spectroscopy of C_{60} Molecules and Clusters in Parahydrogen Solids. *J. Phys. Chem. A* **2000**, *104*, 3733–3742.

(8) Wakabayashi, T.; Momose, T.; Fajardo, M. E. Matrix Isolation Spectroscopy and Spectral Simulations of Isotopically Substituted C_{60} Molecules. *J. Chem. Phys.* **2019**, *151*, 234301.

(9) Stewart, J. T.; Brumfield, B. E.; Gibson, B. M.; McCall, B. J. Inefficient Vibrational Cooling of C_{60} in a Supersonic Expansion. *ISRN Phys. Chem.* **2013**, *2013*, 1–10.

(10) Changala, P. B.; Weichman, M. L.; Lee, K. F.; Fermann, M. E.; Ye, J. Rovibrational Quantum State Resolution of the C_{60} Fullerene. *Science* **2019**, *363*, 49–54.

(11) Nemes, L.; Ram, R. S.; Bernath, P. F.; Tinker, F. A.; Zumwalt, M. C.; Lamb, L. D.; Huffman, D. R. Gas-phase Infrared Emission spectra of C_{60} and C_{70}. Temperature-Dependent Studies. *Chem. Phys. Lett.* **1994**, *218*, 295 – 303.

(12) Schettino, V.; Pagliai, M.; Ciabini, L.; Cardini, G. The Vibrational Spectrum of Fullerene C_{60}. *J. Phys. Chem. A* **2001**, *105*, 11192–11196.

(13) Choi, C. H.; Kertesz, M.; Mihaly, L. Vibrational Assignment of All 46 Fundamentals of C_{60} and C_{60}^{6-}: Scaled Quantum Mechanical Results Performed in Redundant Internal Coordinates and Compared to Experiments. *J. Phys. Chem. A* **2000**, *104*, 102–112.

(14) Cami, J.; Bernard-Salas, J.; Peeters, E.; Malek, S. E. Detection of C_{60} and C_{70} in a Young Planetary Nebula. *Science* **2010**, *329*, 1180–1182.

(15) García-Hernández, D. A.; Manchado, A.; García-Lario, P.; Stanghellini, L.; Villaver, E.; Shaw, R. A.; Szczerba, R.; Perea-Calderón, J. V. Formation of Fullerenes in H-Containing Planetary Nebulae. *Astrophys. J.* **2010**, *724*, L39–L43.

(16) Sellgren, K.; Werner, M. W.; Ingalls, J. G.; Smith, J. D. T.; Carleton, T. M.; Joblin, C. C_{60} in Reflection Nebulae. *Astrophys. J.* **2010**, *722*, L54–L57.

(17) Berné, O.; Cox, N. L. J.; Mulas, G.; Joblin, C. Detection of Buckminsterfullerene Emission in the Diffuse Interstellar Medium. *Astron. Astrophys.* **2017**, *605*, L1.

(18) Zhang, Y.; Kwok, S. Detection of C_{60} in the Protoplanetary Nebula IRAS 01005+7910. *Astrophys. J.* **2011**, *730*, 126.

(19) Gielen, C.; Cami, J.; Bouwman, J.; Peeters, E.; Min, M. Carbonaceous Molecules in the Oxygen-Rich Circumstellar Environment of Binary Post-AGB Stars - C_{60} Fullerenes and Polycyclic Aromatic Hydrocarbons. *Astron. Astrophys.* **2011**, *536*, A54.

(20) García-Hernández, D. A.; Villaver, P., E. García-Lario; Acosta-Pulido, J. A.; Manchado, A.; Stanghellini, L.; Shaw, R. A.; Cataldo, F. Infrared Study of Fullerene Planetary Nebulae. *Astrophys. J.* **2012**, *760*, 107.

(21) Otsuka, M.; Kemper, F.; Cami, J.; Peeters, E.; Bernard-Salas, J. Physical Properties of Fullerene-Containing Galactic Planetary Nebulae. *Mon. Not. R. Astron. Soc* **2014**, *437*, 2577–2593.

(22) Roberts, K. R. G.; Smith, K. T.; Sarre, P. J. Detection of C_{60} in Embedded Young Stellar Objects, a Herbig Ae/Be Star and an Unusual Post-Asymptotic Giant Branch Star. *Mon. Not. R. Astron. Soc* **2012**, *421*, 3277–3285.

(23) Peeters, E.; Tielens, A. G. G. M.; Allamandola, L. J.; Wolfire, M. G. The 15-20 μm Emission in the Reflection Nebula NGC 2023. *Astrophys. J.* **2012**, *747*, 44.

(24) Castellanos, P.; Berné, O.; Sheffer, Y.; Wolfire, M. G.; Tielens, A. G. G. M. C_{60} in Photodissociation Regions. *Astrophys. J.* **2014**, *794*, 83.

(25) Scott, A.; Duley, W. W.; Pinho, G. P. Polycyclic Aromatic Hydrocarbons and Fullerenes as Decomposition Products of Hydrogenated Amorphous Carbon. *Astrophys. J.* **1997**, *489*, L193.

(26) Chuvilin, A.; Kaiser, U.; Bichoutskaia, E.; Besley, N. A.; Khlobystov, A. N. Direct Transformation of Graphene to Fullerene. *Nat. Chem.* **2010**, *2*, 450–453.

(27) Zhen, J.; Castellanos, P.; Paardekooper, D. M.; Linnartz, H.; Tielens, A. G. G. M. Laboratory Formation of Fullerenes from PAHS: Top-Down Interstellar Chemistry. *Astrophys. J.* **2014**, *797*, L30.

(28) Lebeault, M. A.; Baguenard, B.; Concina, B.; Calvo, F.; Climen, B.; LÃĭpine, F.; Bordas, C. Decay of C_{60} by Delayed Ionization and C_2 Emission: Experiment and Statistical Modeling of Kinetic Energy Release. *J. Chem. Phys.* **2012**, *137*, 054312.

(29) Campbell, E. E. B.; Rohmund, F. Fullerene Reactions. *Rep. Prog. in Phys.* **2000**, *63*, 1061–1109.

(30) Biennier, L.; Jayaram, V.; Suas-David, N.; Georges, R.; Singh, M. K.; Arunan, E.; Kassi, S.; Dartois, E.; Reddy, K. P. J. Shock-wave Processing of C_{60} in Hydrogen. *Astron. Astrophys.* **2017**, *599*, A42.

(31) Sommer, T.; Kruse, T.; Roth, P. Thermal Stability of Fullerenes: A Shock Tube Study on the Pyrolysis of C_{60} and C_{70}. *J. Phys. B At. Mol. Phys.* **1996**, *29*, 4955–4964.

(32) Campbell, E. K.; Holz, M.; Gerlich, D.; Mayer, J. P. Laboratory Confirmation of C_{60}^+ as the Career of Two Diffuse Interstellar Bands. *Nature* **2015**, *523*, 322–323.

(33) Cordiner, M. A.; Linnartz, H.; Cox, N. L. J.; Cami, J.; Najarro, F.; Proffitt, C. R.; Lallement, R.; Ehrenfreund, P.; Foing, B. H.; Gull, T. R. et al. Confirming Interstellar C_{60}^+ Using the Hubble Space Telescope. *Astrophys. J.* **2019**, *875*, L28.

(34) Foing, B. H.; Ehrenfreund, P. Detection of Two Interstellar Absorption Bands Coincident with Spectral Feature of C_{60}^+. *Nature* **1994**, *369*, 296–298.

(35) Jenniskens, P.; Desert, F. X. A Survey of Diffuse Interstellar bands (3800-8680 Å). *Astron. Astrophys. Suppl. Ser.* **1994**, *106*, 39–78.

(36) Hobbs, L. M.; York, D. G.; Thorburn, J. A.; Snow, T. P.; Bishof, M.; Friedman, S. D.;

McCall, B. J.; Oka, T.; Rachford, B.; Sonnentrucker, P. et al. Studies of the Diffuse Interstellar Bands. III. HD 183143. *Astrophys. J.* **2009**, *705*, 32–45.

(37) Sarre, P. J. The Diffuse Interstellar Bands: A Major Problem in Astronomical Spectroscopy. *J. Mol. Spectrosc.* **2006**, *238*, 1–10.

(38) Herbig, G. H. The Diffuse Interstellar Bands. *Ann. Rev. Astron. Astrophys.* **1995**, *33*, 19–74.

(39) Joblin, C.; Maillard, J. P.; d'Hendecourt, L.; Léger, A. Detection of Diffuse Interstellar Bands in the Infrared. *Nature* **1990**, *346*, 729–731.

(40) Groh, J. H.; Damineli, A.; Jablonski, F. Spectral Atlas of Massive Stars around He I 10 830 Å. *Astron. Astrophys.* **2007**, *465*, 993–1002.

(41) Geballe, T. R.; Najarro, F.; Figer, D. F.; Schlegelmilch, B. W.; de La Fuente, D. Infrared Diffuse Interstellar Bands in the Galactic Centre Region. *Nature* **2011**, *479*, 200–202.

(42) Cox, N. L. J.; Cami, J.; Kaper, L.; Ehrenfreund, P.; Foing, B. H.; Ochsendorf, B. B.; van Hooff, S. H. M.; Salama, F. VLT/X-Shooter Survey of Near-Infrared Diffuse Interstellar Bands. *Astron. Astrophys.* **2014**, *569*, A117.

(43) Rawlings, M. G.; Adamson, A. J.; Kerr, T. H. A High-Resolution Study of Near-Infrared Diffuse Interstellar Bands. *Astrophys. J.* **2014**, *796*, 58.

(44) Hamano, S.; Kobayashi, N.; Kondo, S.; Sameshima, H.; Nakanishi, K.; Ikeda, Y.; Yasui, C.; Mizumoto, M.; Matsunaga, N.; Fukue, K. et al. Near Infrared Diffuse Interstellar Bands Toward the Cygnus OB2 Association. *Astrophys. J.* **2016**, *821*, 42.

(45) Elyajouri, M.; Lallement, R.; Monreal-Ibero, A.; Capitanio, L.; Cox, N. L. J. Near-Infrared Diffuse Interstellar bands in APOGEE Telluric Standard Star Spectra . Weak bands and Comparisons with Optical Counterparts. *Astron. Astrophys.* **2017**, *600*, A129.

(46) Rawlings, M. G.; Adamson, A. J.; Marshall, C. C. M.; Sarre, P. J. Near-Infrared Diffuse Interstellar Bands towards Her 36. *Mon. Not. R. Astron. Soc.* **2019**, *485*, 3398–3401.

(47) Galazutdinov, G. A.; Lee, J.-J.; Han, I.; Lee, B.-C.; Valyavin, G.; Krełowski, J. Infrared Diffuse Interstellar Bands. *Mon. Not. R. Astron. Soc.* **2017**, *467*, 3099–3104.

(48) Salama, F.; Bakes, E. L. O.; Allamandola, L. J.; Tielens, A. G. G. M. Assessment of the Polycyclic Aromatic Hydrocarbon–Diffuse Interstellar Band Proposal. *Astrophys. J.* **1996**, *458*, 621.

(49) Cox, N. L.J., The PAH-DIB Hypothesis. *EAS Pub. Ser.* **2011**, *46*, 349–354.

(50) Mattioda, A. L.; Hudgins, D. M.; Allamandola, L. J. Experimental Near-Infrared Spectroscopy of Polycyclic Aromatic Hydrocarbons between 0.7 and 2.5 μm. *Astrophys. J.* **2005**, *629*, 1188–1210.

(51) Geballe, T. R.; Joblin, C.; D'Hendecourt, L. B.; Jourdain de Muizon, M.; Tielens, A. G. G. M.; Leger, A. Detection of the Overtone of the 3.3 μm Emission Feature in IRAS 21282+5050. *Astrophys. J.* **1994**, *434*, L15.

(52) García-Hernández, D. A.; Díaz-Luis, J. J. Diffuse Interstellar Bands in Fullerene Planetary Nebulae:The Fullerenes - Diffuse Interstellar Bands Connection. *Astron. Astrophys.* **2013**, *550*, L6.

(53) Sassara, A.; Zerza, G.; Chergui, M.; Leach, S. Absorption Wavelengths and Bandwidths for Interstellar Searches of C_{60} in the 2400-4100 Å Region. *Astrophys. J.* **2001**, *135*, 263–273.

(54) Cami, J. Can Fullerene Analogues be the Carriers of the Diffuse Interstellar Bands? *Proc. Int. Astro. Union* **2013**, *9*, 370–374.

(55) Bakes, E. L. O.; Tielens, A. G. G. M. In *The Diffuse Interstellar Bands*; Tielens, A. G. G. M., Snow, T. P., Eds.; Springer Netherlands: Dordrecht, 1995; pp 315–321.

(56) Louviot, M.; Suas-David, N.; Boudon, V.; Georges, R.; Rey, M.; Kassi, S. Strong Thermal Nonequilibrium in Hypersonic CO and CH_4 Probed by CRDS. *J. Chem. Phys.* **2015**, *142*, 214305.

(57) Dudás, E.; Suas-David, N.; Brahmachary, S.; Kulkarni, V.; Benidar, A.; Kassi, S.; Charles, C.; Georges, R. High-Temperature Hypersonic Laval Nozzle for Non-LTE Cavity Ringdown Spectroscopy. *J. Chem. Phys.* **2020**, *152*, 134201.

(58) Chakraborty, S.; Mulas, G.; Demyk, K.; Joblin, C. Experimental Approach to the Study of Anharmonicity in the Infrared Spectrum of Pyrene from 14 to 723K. *J. Phys. Chem. A* **2019**, *123*, 4139–4148.

(59) Demyk, K.; Meny, C.; Lu, X. H.; Papatheodorou, G.; Toplis, M. J.; Leroux, H.; Depecker, C.; Brubach, J. B.; Roy, P.; Nayral, C. et al. Low Temperature MIR to Submillimeter Mass Absorption Coefficient of Interstellar Dust Analogues. I. Mg-rich Glassy Silicates. *Astron. Astrophys.* **2017**, *600*, A123.

(60) Procacci, P.; Berne, B. J. Computer Simulation of Solid C_{60} using Multiple Time-Step Algorithms. *J. Chem. Phys.* **1994**, *101*, 2421–2431.

(61) Love, S.; McBranch, D.; Salkola, M.; Coppa, N.; Robinson, J.; Swanson, B.; Bishop, A. Near-infrared Raman spectroscopy of Solid C_{60}. Raman Activation of Silent Modes by ^{13}C and Sample Disorder. *Chem. Phys. Lett.* **1994**, *225*, 170 – 180.

(62) AnharmonicIPR20. https://sourceforge.net/projects/anharmonic-ipr-20/.

(63) Atkins, P.; Friedman, R. *Molecular Quantum Mechanics: Fourth Edition*; Oxford University Press Inc., New York, 2005.

(64) Narasimhan, L. R.; Stoneback, D. N.; Hebard, A. F.; Haddon, R. C.; Patel, C. K. N. Infrared Spectroscopy Through the Orientational Phase Transition in Fullerene Films. *Phys. Rev. B* **1992**, *46*, 2591–2594.

(65) van Loosdrecht, P. H. M.; van Bentum, P. J. M.; Meijer, G. Rotational Ordering Transition in Single-Crystal C_{60} Studied by Raman spectroscopy. *Phys. Rev. Lett.* **1992**, *68*, 1176–1179.

(66) Menéndez, J.; Page, J. B. In *Light Scattering in Solids VIII: Fullerenes, Semiconductor Surfaces, Coherent Phonons*; Cardona, M., Güntherodt, G., Eds.; Springer Berlin Heidelberg: Berlin, Heidelberg, 2000; pp 27–95.

(67) Brieva, A.; Gredel, R.; Jäger, C.; Huisken, F.; Henning, T. C_{60} As a Probe for Astrophysical Environments. *Astrophys. J.* **2016**, *826*, 122.

Graphical TOC Entry